http://dx.doi.org/10.5012/bkcs.2013.34.8.2321

Effects of Ligand-exchanged Cadmium Selenide Nanoparticles on the Performance of P3HT:PCBM:CdSe Ternary System Solar Cells

Eung-Kyu Park, Honghong Fu,† Mijung Choi,‡ Weiling Luan,† and Yong-Sang Kim*

School of Electronic and Electrical Engineering, Sungkyunkwan University, Gyeonggi 440-746, Korea
**E-mail: yongsang@skku.edu*
†School of Mechanical and Power Engineering, East China University of Science and Technology, Shanghai 200237, China
‡MLB Lab, Korea circuit Co. Ltd, Ansan, Gyeonggi 425-833, Korea
Received April 9, 2013, Accepted May 10, 2013

An improved hybrid solar cell was obtained by focusing on the effects of ligand for CdSe nanoparticles, in the active layers. The performance was compared by mixing nanoparticles capped with pyridine or oleic acid for the acceptor material into poly(3-hexylthiophene):[6,6]-phenyl C61 butyric acid methyl ester based active layer. The solar cells with pyridine capped CdSe nanoparticles showed a power conversion efficiency of 2.96% while oleic acid capped CdSe nanoparticles showed 2.85%, under AM 1.5G illumination. Formation of percolation pathways for carrier transport and a reduction in the hopping event resulted in better performance of pyridine capped nanoparticles.

Key Words : CdSe NPs, Ligand-exchange, Organic solar cell, Ternary system

Introduction

Organic Solar Cells (OSCs) based on conjugated polymer and fullerene bulk heterojunction (BHJ) are one of the most attractive area of study for renewable energy source; for their advantages like light-weight, flexibility, low-cost, and simple fabrication for large processing area. Among the various conductive polymers: high electron mobility and high light absorption coefficient in the visible region make polythiophenes a promising candidate as electron donor materials for OSCs. Recent studies have reported remarkably improved performances of the BHJ solar cells up to 5% of power conversion efficiency (PCE) with poly(3-hexylthiophene):[6,6]-phenyl C61 butyric acid methyl ester (P3HT:PCBM).[1] The performance of OSCs is affected by the active layer characteristics such as optical absorbance, chemical properties, phase separation and morphology. For increased performance, many researchers have optimized processing conditions such as solvent, annealing temperature and time, composition mixture ratio in solvent.[2-5] However in the polymer and fullerene blend, the PCE of the devices are limited as the charge carrier mobility is comparatively low with a short exciton diffusion length in the active layer.[6] In order to improve the performance of OSCs, it is required to introduce other additive materials. A promising approach to improve light absorption without increasing photoactive layer thickness is to trap light in the active layer using quantum dots (QDs) based on inorganic semiconductor such as CdSe Nanoparticles (NPs). These NPs can be dispersed with polymer in solvent and then be solution processed. The inorganic semiconductors have much better electronic properties of enhanced light harvesting capabilities in the long wavelength region of the solar spectrum. In addition, the band gap and properties of QDs can be easily tuned by the change in size or addition of ligand during synthesis. Various research groups have so far studied on hybrid solar cells using organic and inorganic materials such as CdSe NPs.[7,8]

By ligand exchange, solubility of the nanoparticles in special solvents can be obtained, new functional groups can be introduced onto the surface, or the thickness of the ligand shell can be reduced. An exchange of the original ligand shell by smaller molecules is especially important for applications based on charge transfer between nanoparticles, since long carbon chains bound to the surface of nanoparticles form a barrier to charge carriers.

In this regard, we fabricated a CdSe NPs based ternary hybrid solar cells; and compared and optimized the properties by exchanging the CdSe ligands. The device was characterized by measuring the optical and electrical properties.

Experimental

We fabricated the solar cell devices with the structure of FTO/TiO_2/P3HT:PCBM:CdSe/PEDOT:PSS/Ag as shown in Figure 1(a). CdSe NPs were synthesized according to the procedure prescribed by Yang *et al.*[9] We used two types of ligands in this work for comparison, namely, ring shaped-pyridine and long chain fatty acid- oleic acid (OA) for comparison. OA ligands were replaced with pyridine by stirring the NPs in an excess of anhydrous pyridine at 65 ºC for 3 h. Thereafter, CdSe/pyridine solution was stirred at room temperature for 24 h. The device was fabricated and characterized according to the previously published report.[10] In short, the CdSe NPs mixed with P3HT:PCBM (30 mg/mL) (P3HT:PCBM:CdSe=1:1:0.1 weight ratio) in chlorobenzene solvent were spin coated on TiO_2 coated FTO sub-

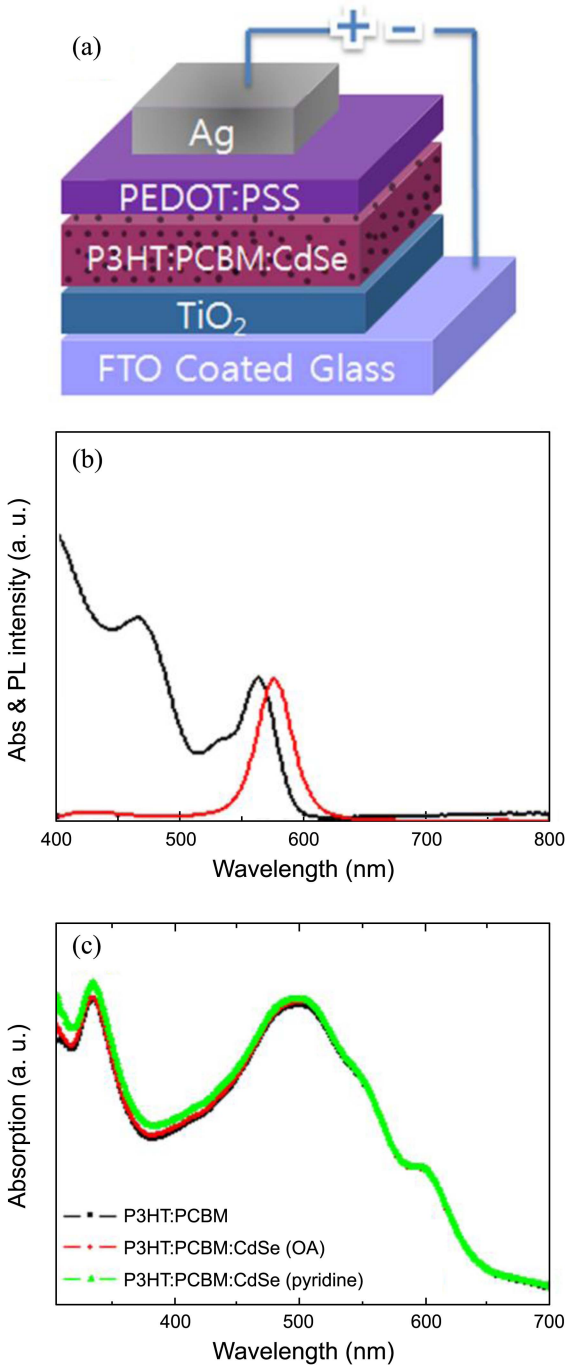

Figure 1. The schematic of inverted hybrid solar cell. (b) UV/visible absorption and photoluminescence spectra of the synthesized CdSe NPs. (c) UV/visible spectra of P3HT:PCBM and P3HT:PCBM:CdSe films after annealing at 160 ºC for 5 min.

strate. Hydrophilic PEDOT:PSS was mixed with 0.5 vol % of Triton X-100 and spin coated on a hydrophobic active layer with a hexamethylene disilazane a layer in between them. After thermal pre-annealing conducted at 160 ºC for 5 min on a hot plate in ambient air, the Ag top electrode (100 nm) was deposited on PEDOT:PSS layer by thermal evaporation, defining an active area of 0.1 cm^2. The hybrid solar cells were characterized in the air without any encapsulation. The current density-voltage (J-V) characteristics were measured with J-V curve tracer (Eko MP-160) and solar simulator (Yss-E40, Yamashita Denso) under AM 1.5G (100 mW/cm^2) irradiation intensity.

Results and Discussion

The UV/visible absorption and photoluminescence spectra of the synthesized CdSe NPs is shown in Figure 1(b). From the absorption spectra, the diameter of the particle can be predicted using equation proposed by Yu *et al.* The size of CdSe NPs was calculated to be around 3.3 nm from the maximum wavelength, 563 nm, of CdSe NPs absorption peak (λ_{max}).

The crystallization of P3HT tends to be disturbed when increasing amounts of PCBM is blended in active layer.[11,12] Since CdSe, has a similar tendency,[8] the composition of the active layer in solvent is important for optimum performance. For these reasons, we optimized the amount of CdSe NPs (10 wt % of P3HT) in the present work. The role of capping the ligands in NPs is to prevent aggregation, and the electrical properties are dominated by capped ligands. The ligands act as an insulator or a carrier trap site that interrupts carrier transport from the active layer to electrode.[13] In the past we also reported that the inverted structure using fluorine-doped tin oxide (FTO) can improve the device performances with higher stability and efficiency.[14] Figure 1(c) shows the UV/visible absorption spectra of the P3HT:PCBM and P3HT:PCBM:CdSe (with different ligands) active layer films after annealing at 160 ºC for 5 min. The overall absorption spectra of pristine active layer is overlapped with CdSe NPs contained active layer. The thickness of active layer was 75 nm in these cases. Addition of CdSe NPs did not affect the thickness of the active layer film, as the spin speed was optimized to control the thickness. As per the previous reports, absorption spectrum of P3HT is known to increase and become broader with a red-shift after annealing due to crystallization of P3HT in active layer.[5] The surface modification procedure did not alter the absorption peak position, indicating that the size of the NPs did not change during ligand exchange. However, TEM images of the corresponding samples demonstrate some changes (Fig. 2).

Figure 2 shows the TEM images of the active layer. Figure 2(a) is a TEM image of active layer without CdSe NPs. We can observe a uniformly distributed crystallization in the active layer. As seen in Figure 2(b), OA capped CdSe NPs are well dispersed in the active layer film. The long-chained OA prevented the aggregation of NPs in the active layer. Figure 2(c) shows the TEM image of active layer with pyridine capped CdSe NPs aggregated in the active layer. Though the size of aggregation is over 50 nm, absolute size of NPs did not change due to smaller chemical structure of pyridine.

The measured J-V characteristics of hybrid solar cells using P3HT:PCBM, P3HT:PCBM:CdSe (OA) and P3HT:PCBM:CdSe (pyridine) are shown in Figure 3(a). It can be observed that the highest performance of hybrid solar cells was shown by P3HT:PCBM:CdSe (pyridine). The exciton generation was proportionate to light absorption in the active

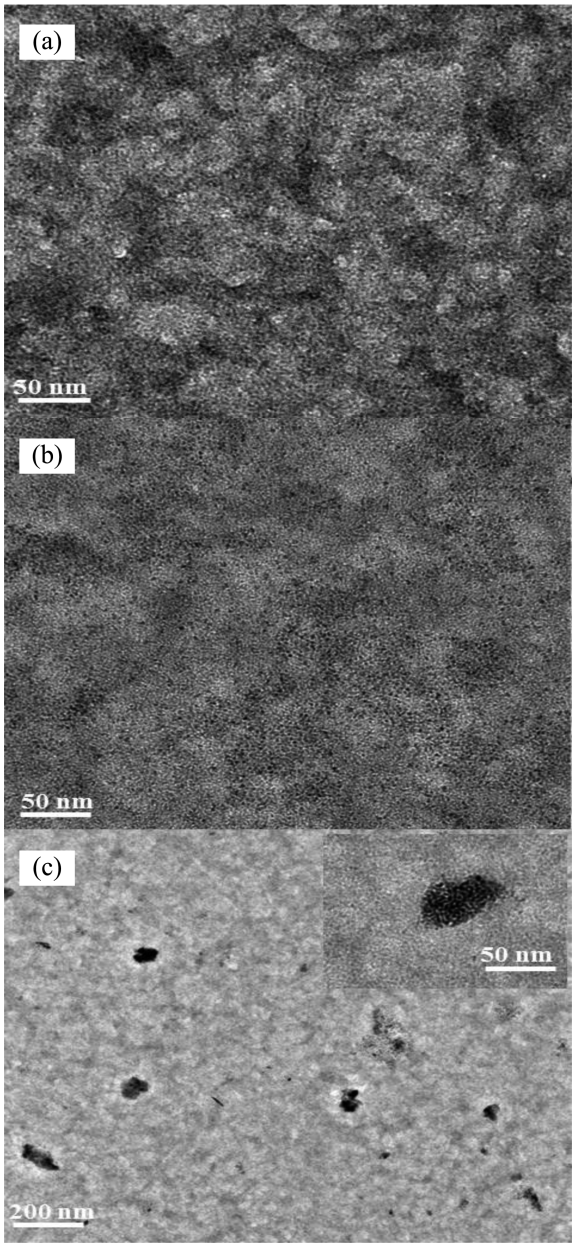

Figure 2. TEM images of active layer of films prepared under the identical condition. (a) P3HT:PCBM. (b) P3HT:PCBM:CdSe (OA). (c) P3HT:PCBM:CdSe (pyridine).

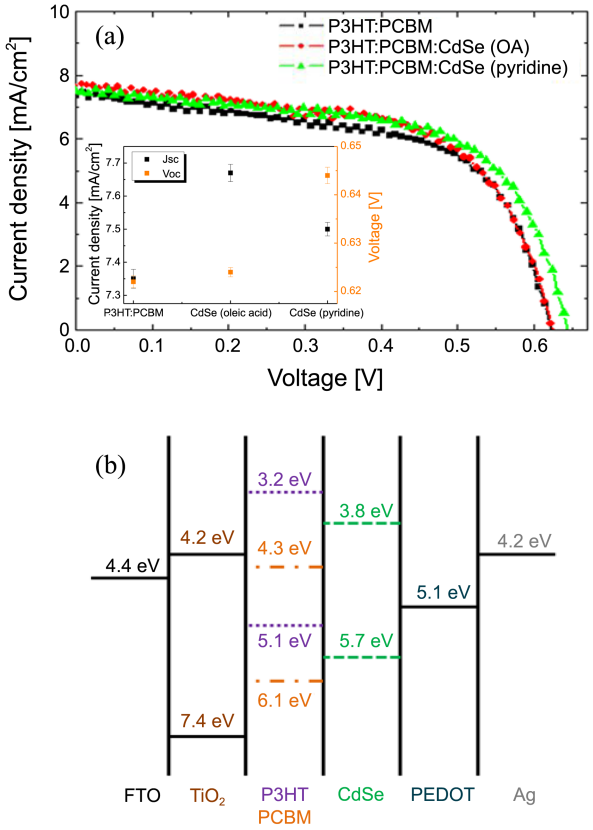

Figure 3. (a) J-V characteristics of hybrid solar cells with P3HT:PCBM layer, P3HT:PCBM:CdSe (OA) layer, and P3HT:PCBM:CdSe (pyridine) layer at an irradiation intensity of 100 mW/cm^2 (Inset: standard deviation of output) (b) Energy band structure of BHJ solar cell.

layer. This suggests that pyridine capped CdSe NPs in P3HT:PCBM:CdSe ternary system can initiate percolation pathways for carrier transport and therefore reduce the hopping event between NPs and polymer or NPs and NPs without changing the shape of CdSe NPs into rods or branched structure. Consequently, FF is also improved as the thin film resistivity is decreased. Recently, N. T. N. Truong *et al.*[8] suggested that the critical loading amount of CdSe/P3HT composite provides a decrease in thin film resistivity and increase in device efficiency which support the possible development of the electrical percolation pathways at the critical loading amount of CdSe/P3HT composite. Figure 3(a) inset shows the standard deviation of results of different devices (n = 3). Small error bars proves the stability and reproducibility of our experiment. Figure 3(b) illustrates the energy band diagram of active layer with CdSe NPs. Since the size does not alter after ligand change, same diagram can be used for the ligand exchanged CdSe Nps.[15]

The performance of all the hybrid solar cells is summarized in Table 1. Generally high absorption of light results in high current density, but in our case, oleic-acid capped CdSe NPs showed the highest current density. Because the size of OA capped CdSe NPs is just 3.3 nm, it helped in the fast electron transfer resulting in highest current density measured.[16,17] The improved performance of P3HT: PCBM: CdSe (pyridine) device can be attributed to the use of CdSe NPs with pyridine capping. Pyridine capped CdSe NPs helped in formation of better percolation pathway for the

Table 1. Device performance of hybrid solar cells with P3HT:PCBM layer, P3HT:PCBM:CdSe (OA) layer and P3HT:PCBM:CdSe (pyridine) layer

Active layer	J_{sc} [mA/cm^2]	V_{oc} [V]	PCE [%]	F.F.
P3HT:PCBM	7.35	0.622	2.74	0.59
P3HT:PCBM:CdSe (OA)	7.67	0.624	2.85	0.59
P3HT:PCBM:CdSe (pyridine)	7.50	0.644	2.96	0.61

carrier transport and reducing the hopping event. It is well-known that dangling bonds on Cd and pyridine bound Cd, i.e. unpassivated surface sites lead to deep electron and hole traps respectively.[19] It is also established that the aromatic ring can efficiently stabilize a positive charge.[18] Pyridine-treated CdSe NPs tend to form aggregates within the blends.[17] The holes get localized at pyridine molecules located at surface regions inside of CdSe aggregates, *i.e.*, at regions spatially separated from the polymer phase. The hole transfer to the polymer should become poorly efficient; instead, nonradiative recombination in the NPs occurs as a loss mechanism. As a consequence, light absorption in the nanoparticle phase gives only a limited contribution to the photocurrent in the case of the pyridine-based system.[19] For these reasons pyridine capped CdSe NPs showed increased Voc (Fig. 1(c)) but low current density. In explanation, the CdSe NPs changes the LUMO level of the device.

Conclusion

We investigated the effect of ligand exchanged CdSe NPs in P3HT:PCBM:CdSe ternary system. After ligand-exchange, the size of oleic acid capped CdSe NPs did not change and showed highest current density due to faster electron transfer. On the other side, pyridine capped CdSe NPs aggregated well in the active layer and provided the percolation pathway for charge transport in the active layer. Cd dangling bonds acted as an electron trap, and pyridine bonded to the surface of Cd atoms introduced hole traps. Due to the reduced hopping event during charge transport, introduction of pyridine capped CdSe NPs in P3HT:PCBM organic solar cell showed the highest PCE.

References

1. Kim, K.; Liu, J.; Namboothiry, M. A. G.; Carroll, D. L. *Appl. Phys. Lett.* **2007**, *90*, 163511.
2. Yang, X.; Loos, J.; Veenstra, S. C.; Verhees, W. J.; Wienk, M. M.; Kroon, M. J.; Michels, M. A. J.; Janssen, R. A. *J. Nono Lett.* **2005**, *5*, 579.
3. Kim, Y.; Choulis, S. A.; Nelson, J.; Cook, S.; Bradley, D. D. C.; Durrant, J. R. *Appl. Phys. Lett.* **2005**, *86*, 063502.
4. Baek, W. H.; Yang, H.; Yoon, T. S.; Kang, C. J.; Lee, H. H.; Kim, Y. S. *Sol. Energy Mater. Sol. Cells* **2009**, *90*, 1263.
5. Li, G.; Yao, Y.; Yang, H.; Shirotriya, V.; Yang, G.; Yang, Y. *Adv. Funct. Mater.* **2007**, *17*, 1636.
6. Coakley, K. M.; McGehee, M. D. *Chem. Mater.* **2004**, *16*, 4533.
7. Huynh, W. U.; Dittmer, J. J.; Alivisatos, A. P. *Science* **2002**, *295*, 2425.
8. Truong, N. T. N.; Kim, W. K.; Park, C. *Sol. Energy Mater. Sol. Cells* **2011**, *95*, 167.
9. Yang, H.; Luan, W.; Tu, S.; Wang, Z. M. *Crystal Growth and Design.* **2009**, *9*, 1569.
10. Fu, H.; Choi, M.; Luan, W.; Kim, Y. S.; Tu, S. T. *Solid-State Electronics* **2012**, *69*, 50.
11. Vanlaeke, P.; Swinnen, A.; Haeldermans, I.; Vanhoyland, G.; Aernouts, T.; Cheyns, D.; Deibel, C.; D'Heaen, J.; Heremans, P.; Poortmans, J.; Manca, J. V. *Sol. Energy Mater. Sol. Cells* **2006**, *90*, 2150.
12. Baek, W. H.; Yoon, T. S.; Lee, H. H.; Kim, Y. S. *Organic Electronics* **2010**, *11*, 933.
13. Kalyuzhny, G.; Murray, R. W. *J. Phys. Chem. B* **2005**, *109*, 7012.
14. Baek, W. H.; Choi, M.; Yoon, T. S.; Lee, H. H.; Kim, Y. S. *Appl. Phys. Lett.* **2010**, *96*, 133506.
15. Bang, J. H.; Kamat, P. V. *American Chemical Society* **2011**, *5*, 9421.
16. Lokteva, I.; Radychev, N.; Witt, F.; Borchert, H.; Parisi, J.; Kolny-Olesiak, J. *Phys. Chem. C* **2010**, *114*, 12784.
17. Derbal-Habak, H.; Bergeret, C.; Cousseau, J.; Nunzi, J. M. *Sol. Energy Mater. Sol. Cells* **2011**, *95*, S53.
18. Klimov, V. I. J. *Phys. Chem. B* **2000**, *104*, 6112.
19. Radychev, N.; Lokteva, I.; Witt, F.; Kolny-Olesiak, J.; Borchert, H.; Parisi, J. *Phys. Chem. C* **2011**, *115*, 14111.